

## Phase conjugation with a single bubble

Valentin Leroy,<sup>\*</sup> Jean-Claude Bacri,<sup>†</sup> Thierry Hocquet,<sup>‡</sup> and Martin Devaud<sup>§</sup>

Laboratoire Matière et Systèmes Complexes, Université Denis Diderot—Paris 7, 140 rue de Lourmel, 75015 Paris, France

(Received 20 January 2005; published 4 October 2005)

It is recalled how the nonlinear interaction between a gas bubble and an external extra pressure can yield phase conjugation. Using the Glauber representation, we show that the effect of the latter is formally analogous to that of a  $\pi$  pulse in nuclear magnetic resonance, so that the acoustic equivalent of spin echoes may be expected in a bubble cloud. An experimental attempt to observe phase conjugation is reported in the single-bubble case.

DOI: [10.1103/PhysRevE.72.046601](https://doi.org/10.1103/PhysRevE.72.046601)

PACS number(s): 43.20+g, 43.25+y, 43.60+d

### I. INTRODUCTION

First observed in the optics domain, many nonlinear effects have been successfully transposed in the acoustics field [1]. In the latter field, the most frequently cited (if not used) nonlinear medium is undoubtedly the bubbly liquid. Injecting gas bubbles in a liquid provides it indeed with a strong acoustical nonlinearity. In the eighties, the phase conjugation of a sound wave traveling through a bubbly liquid was theoretically studied [2,3] and experimentally observed [4–6]. Other nonlinear phenomena, such as Raman scattering for instance [7], were also observed. Recently, bubbles have also been proposed as an active medium for the practical implementation of an acoustic laser [8]. Nonlinear properties of bubbles are also of great interest for medical purposes: harmonic imaging, with bubbles as contrast agent, is a major field of ultrasonic echography.

In the present paper, we report the evidence of a phase conjugation effect with a *single* bubble.

Section II is devoted to the theoretical formulation of this question. Introducing a complex variable allowing by itself for the bubble's physical state enables us to use the secular approximation and get simplified motion equations. Two particular cases are then considered and solved: the direct and parametric resonant excitations. It is shown that the latter excitation involves phase conjugation. In Sec. III, we propose an experimental check of this phase conjugation effect with a single bubble. Taking advantage of the specific phase signature of the conjugated component of the oscillation, we perfect a lock-in phase detection procedure to extract this conjugated component from the background linear component. Lastly, in Sec. IV, we demonstrate the analogy between the phase conjugation of one bubble's oscillation and the  $\pi$ -pulse inducing a spin-flip in the NMR domain, and we discuss the possibility of observing bubble echoes in a bubble cloud.

### II. THEORY

Let us consider a spherical air bubble in water, with equilibrium radius  $R_0$  under pressure  $P_0$ , submitted to an extra pressure  $p_e(t)$ . We will study the oscillations of the bubble, using the following approximations. First, we assume that the oscillating bubble remains spherical and that the variation  $\xi(t)$  of its radius is always small compared with  $R_0$ . We also neglect viscosity, surface tension and the compressibility of water. Lastly, we consider that the transformations undergone by the air during the oscillations are isentropic. Note that, as strong as they may seem, these approximations will be valid for the experiments we present in Sec. III.

#### A. Hamiltonian of the bubble

Let us construct a Hamiltonian for the bubble. Three energy terms are involved: potential energy of the gas, kinetic energy of the water, and coupling energy due to the extra pressure.

Since the air inside the bubble is assumed to undergo isentropic transformations, when the radius of the bubble varies from  $R_0$  to  $R_0 + \xi$ , the inner pressure  $P_0$  becomes  $P_0 + p(\xi)$  with extra pressure  $p(\xi)$  given by Laplace's law:

$$\frac{p(\xi)}{P_0} = \left(1 + \frac{\xi}{R_0}\right)^{-3\gamma} - 1, \quad (1)$$

where  $\gamma$  is the air heat capacities ratio [16]. Hence the elastic potential energy associated with the variation of the bubble's radius:

$$\begin{aligned} E_p(\xi) &= - \int_0^\xi d\xi' 4\pi(R_0 + \xi')^2 p(\xi') \\ &= 4\pi P_0 R_0^3 \left[ \frac{\left(1 + \frac{\xi}{R_0}\right)^3 - 1}{3} - \frac{\left(1 + \frac{\xi}{R_0}\right)^{3-3\gamma} - 1}{3-3\gamma} \right]. \end{aligned} \quad (2)$$

Moreover, the total kinetic energy of the surrounding water, assumed incompressible with (constant) mass density  $\rho$ , is given by

<sup>\*</sup>Present address: Laboratoire Ondes et Acoustique, Université Denis Diderot—Paris 7, ESPCI, 10 rue Vauquelin, 75005 Paris, France. Electronic address: valentin.leroy@loa.espci.fr

<sup>†</sup>Electronic address: jcbac@ccr.jussieu.fr

<sup>‡</sup>Electronic address: Thierry.Hocquet@cicrp.jussieu.fr

<sup>§</sup>Electronic address: devaud@ccr.jussieu.fr

$$E_K(\xi, \dot{\xi}) = \frac{1}{2} M_0 \left( 1 + \frac{\xi}{R_0} \right)^3 \dot{\xi}^2, \quad (3)$$

with  $M_0 = 4\pi\rho R_0^3$ . As a consequence, the Lagrangian  $L_0$  of the *free* bubble reads, neglecting air's inertia:

$$L_0(\xi, \dot{\xi}) = E_K(\xi, \dot{\xi}) - E_P(\xi). \quad (4)$$

If now the air bubble is submitted to an outer extra pressure  $p_e(t)$ , Lagrangian  $L_0$  should be substituted by

$$L(\xi, \dot{\xi}, t) = L_0 - \frac{4}{3} \pi R_0^3 \left( 1 + \frac{\xi}{R_0} \right)^3 p_e(t). \quad (5)$$

Introducing the dimensionless variables  $x = \xi/R_0$  and  $y(t) = p_e(t)/P_0$ , this Lagrangian is Legendre-transformed into the Hamiltonian:

$$H(x, p, t) = \frac{p^2}{2I_0} (1+x)^{-3} + \frac{I_0 \omega_0^2}{9\gamma} \left\{ (1+x)^3 - 1 + \frac{(1+x)^{3-3\gamma} - 1}{1-\gamma} + (1+x)^3 y(t) \right\}, \quad (6)$$

with  $I_0 = M_0 R_0^2$ ,  $\omega_0 = \sqrt{3\gamma P_0 / \rho R_0^2}$  the Minnaert angular frequency [9] and where  $p = I_0 (1+x)^3 \dot{x}$  stands for the conjugate momentum of dynamical variable  $x$ . Note that the above Hamiltonian leads to the well-known Rayleigh-Plesset equation (see Ref. [10], p. 302). In the case of small oscillations ( $|x|$  and  $|y| < 1$ ),  $H$  can be considered as the sum of three terms:

$$H = H_0 + W + H_e(t), \quad (7a)$$

with

$$H_0 = \frac{p^2}{2I_0} + \frac{1}{2} I_0 \omega_0^2 x^2, \quad (7b)$$

$$W = \frac{p^2}{2I_0} (-3x + \dots) + \frac{1}{2} I_0 \omega_0^2 ((1-\gamma)x^3 + \dots), \quad (7c)$$

$$H_e(t) = I_0 \omega_0^2 (1 + 3x + 3x^2 + x^3) \frac{y(t)}{9\gamma}. \quad (7d)$$

The first two terms concern the free bubble:  $H_0$  is the harmonic oscillator (HO) Hamiltonian, whereas  $W$  (hereabove expanded in increasing powers of  $x$ ) includes all the nonlinearities of the free oscillator. The third term  $H_e(t)$  is the {bubble-external extra pressure} interaction Hamiltonian.

### B. The Glauber variable

Let us introduce the complex variable  $\alpha$ :

$$\alpha = \frac{1}{\sqrt{2}} \left( x + i \frac{p}{I_0 \omega_0} \right). \quad (8a)$$

Since it gathers both  $x$  and  $p$ , this variable sums up by itself the whole physical state of the oscillator and turns out to be very handy. Indeed,  $\alpha$  obeys a complex and first order dynamic equation instead of the usual real second order equa-

tion. Dealing with first order equations permits us to use secular approximations, hence obtaining very simple equations. Observe that  $\alpha$  is proportional to the variable  $\alpha_{GI}$  first introduced by Glauber in the quantum mechanics domain when aiming at describing the quasiclassical (coherent) states of the HO [11].

We have, as a consequence of (8a):

$$x = \frac{\alpha + \alpha^*}{\sqrt{2}}, \quad p = -i I_0 \omega_0 \frac{\alpha - \alpha^*}{\sqrt{2}}, \quad (8b)$$

and,  $\{ \}$  standing for the Poisson's brackets,

$$\{x, p\} = 1 \rightsquigarrow \{\alpha, \alpha^*\} = \frac{1}{i I_0 \omega_0}. \quad (8c)$$

With the above expressions, Hamiltonians  $H_0$ ,  $W$ , and  $H_e(t)$  respectively read

$$H_0 = I_0 \omega_0^2 |\alpha|^2, \quad (9a)$$

$$W = \frac{I_0 \omega_0^2}{4\sqrt{2}} \{ 3(\alpha - \alpha^*)^2 (\alpha + \alpha^*) + (1-\gamma)(\alpha + \alpha^*)^3 + \dots \}, \quad (9b)$$

$$H_e(t) = I_0 \omega_0^2 \left\{ 1 + \frac{3}{\sqrt{2}} (\alpha + \alpha^*) + \frac{3}{2} (\alpha + \alpha^*)^2 + \frac{1}{2\sqrt{2}} (\alpha + \alpha^*)^3 \right\} \frac{y(t)}{9\gamma}. \quad (9c)$$

### C. Excitation of the bubble

From now on, we shall limit the expansion of Hamiltonian  $H$  to the third order [ $y(t)$  and  $\alpha$  being considered of the same order]. Then, including a phenomenological damping rate  $\Gamma$  to account for dissipation processes, we obtain a time evolution of variable  $\alpha$  ruled by

$$\begin{aligned} \dot{\alpha} = & \left( -i\omega_0 - \frac{\Gamma}{2} \right) \alpha \\ & - i\omega_0 \left( -\frac{3\gamma}{4\sqrt{2}} \alpha^2 - \frac{3\gamma}{2\sqrt{2}} \alpha \alpha^* + \frac{3(4-\gamma)}{4\sqrt{2}} \alpha^{*2} \right) \\ & - i\omega_0 \left( \frac{1}{\sqrt{2}} + \alpha + \alpha^* \right) \frac{y(t)}{3\gamma}. \end{aligned} \quad (10)$$

From Eq. (10) above, two kinds of excitation of the bubble's oscillations can be envisaged. To see it, let us consider the nonlinear terms as well as the  $y(t)$  terms in the right-hand side as small perturbations, and set up a perturbative resolution of this equation. Obviously, the unperturbed time evolution of  $\alpha$  is

$$\alpha^{(0)}(t) = A e^{-i\omega_0 t} e^{-(\Gamma/2)t}, \quad (11)$$

with  $A = \alpha^{(0)}(t=0)$ . In order to take the perturbation into account, let us allow constant  $A$  to vary with time and set

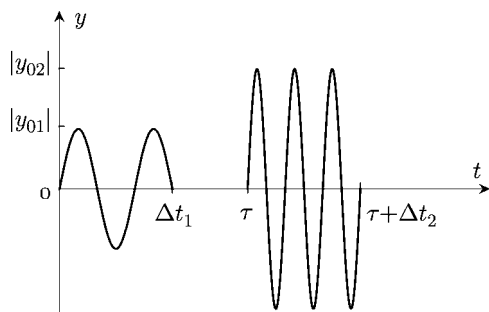


FIG. 1. The two-pulse sequence used to excite the bubble. The first pulse (with angular frequency  $\omega_1 \approx \omega_0$ ) induces a direct excitation. The second pulse (with  $\omega_2 \approx 2\omega_0$ ) induces a parametric excitation involving the phase conjugation.

$$\alpha(t) = A(t)e^{-i\omega_0 t} e^{-(\Gamma/2)t}. \quad (12)$$

Then, using (12), Eq. (10) becomes

$$\begin{aligned} \dot{A} = & -i\omega_0 \frac{3}{2\sqrt{2}} e^{-(\Gamma/2)t} \\ & \times \left( -\frac{\gamma}{2} A^2 e^{-i\omega_0 t} - \gamma A A^* e^{i\omega_0 t} + \frac{(4-\gamma)}{2} A^{*2} e^{3i\omega_0 t} \right) \\ & - i\omega_0 \left( \frac{1}{\sqrt{2}} e^{i\omega_0 t + (\Gamma/2)t} + A + A^* e^{2i\omega_0 t} \right) \frac{y(t)}{3\gamma}. \end{aligned} \quad (13)$$

In the general case, Eq. (13) above is not easy to solve. Nevertheless, for excitations of the form  $y(t) = \text{Re}\{y_0 e^{-i\omega t}\} = |y_0| \cos(\omega t + \varphi)$ , two resonances appear, respectively for  $\omega = \omega_0$  and  $\omega = 2\omega_0$ .

(i) The  $\omega = \omega_0$  resonance is associated with the *direct* excitation of the air bubble. For  $|\omega - \omega_0| \ll \omega_0$ , and neglecting the nonresonant terms (i.e., at the secular approximation), Eq. (13) simplifies in

$$\dot{A} = -\frac{i\omega_0 y_0}{\sqrt{2} 6\gamma} e^{i(\omega_0 - \omega)t + (\Gamma/2)t}. \quad (14)$$

(ii) The  $\omega = 2\omega_0$  resonance is associated with the *parametric* excitation of the air bubble. For  $|\omega - 2\omega_0| \ll \omega_0$ , and neglecting again the nonresonant terms, Eq. (13) becomes

$$\dot{A} = -i\omega_0 \frac{y_0}{6\gamma} A^* e^{i(2\omega_0 - \omega)t}. \quad (15)$$

Note that Eq. (15) involves a phase conjugation effect: the increase of  $A$  between times  $t$  and  $t+dt$  is proportional to  $A^*$ . Let us now suppose that we excite a bubble with the two-pulse sequence displayed in Fig. 1: a first pulse at  $\omega_1 \approx \omega_0$  (direct excitation), and a second pulse at  $\omega_2 \approx 2\omega_0$  (parametric excitation).

We note  $y_1(t) = |y_{01}| \cos(\omega t + \varphi_1)$  the first acoustic pulse, applied to the bubble between times  $t=0$  and  $t=\Delta t_1$ . If  $|\omega_0 - \omega_1 - i(\Gamma/2)|\Delta t_1 \ll 1$ , the subsequent oscillation (i.e., for  $t > \Delta t_1$ ) is then characterized by the complex variable

$$\alpha_1(t) = -\frac{i}{\sqrt{2}} \frac{|y_{01}|}{6\gamma} \omega_0 \Delta t_1 e^{-i(\omega_0 t + \varphi_1) - (\Gamma/2)t}. \quad (16)$$

The second acoustic pulse, with angular frequency  $\omega_2 \approx 2\omega_0$  and complex amplitude  $y_{02} = |y_{02}| e^{-i\varphi_2}$ , is applied between times  $\tau$  and  $\tau + \Delta t_2$ . Assuming that  $A$  does not vary too much during this second pulse, Eq. (15) is integrated in

$$A(\tau < t < \tau + \Delta t_2) = A_1 - i\omega_0 A_1^* \frac{y_{02}}{6\gamma} \frac{e^{i(2\omega_0 - \omega_2)t} - e^{i(2\omega_0 - \omega_2)\tau}}{i(2\omega_0 - \omega_2)}. \quad (17)$$

Now, assuming that the timewidth and the detuning of this second pulse are such that  $|2\omega_0 - \omega_2|\Delta t_2 \ll 1$ , the subsequent (i.e., for  $t > \tau + \Delta t_2$ ) oscillation of the bubble is described by the complex variable

$$\alpha_{1+2}(t) = \alpha_1(t) + \alpha_{pc}(t), \quad (18)$$

with  $\alpha_1(t)$  displayed in (16) and

$$\alpha_{pc}(t) = \frac{-i}{\sqrt{2}} \frac{|y_{01} y_{02}|}{(6\gamma)^2} \omega_0^2 \Delta t_1 \Delta t_2 e^{-i(\omega_0(t-2\tau) + \omega_2\tau + \varphi_2 - \varphi_1) - (\Gamma/2)t}. \quad (19)$$

Equation (19) deserves some comments. We postpone them to Sec. IV and explain, in the following section, how the phase-conjugated (pc) component of the bubble's oscillation can be experimentally extracted from the overall signal.

### III. EXPERIMENT

Figure 2 displays the experimental setup used to acquire

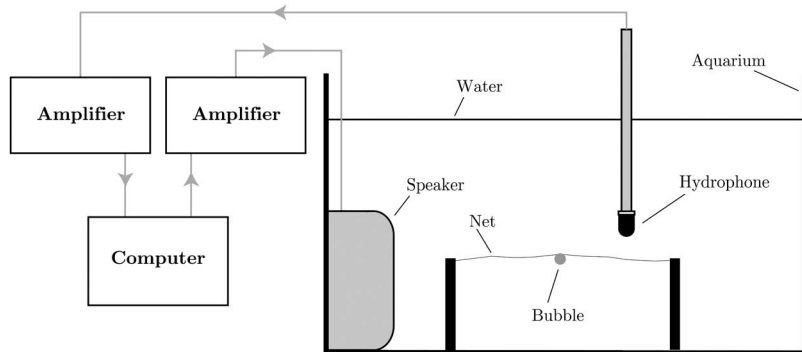


FIG. 2. Sketch of the experimental setup. The bubble, caught under a net, is excited by a two-pulse acoustic sequence generated by a speaker, and its response is detected with a hydrophone.

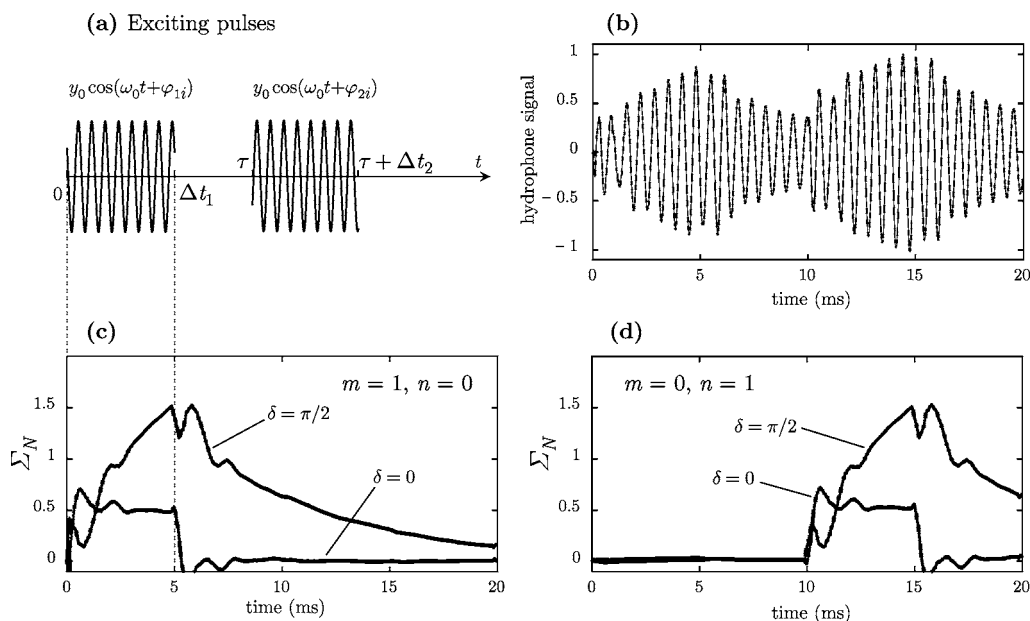


FIG. 3. Illustration and check of the phase detection method. (a) The bubble is excited with  $N$  sequences of two  $\omega_0$ -oscillating pulses bearing the random phases  $\varphi_{1i}$  and  $\varphi_{2i}$ . (b) The measurement of the hydrophone's pressure gives the superposition of the two exciting pulses and the two responses of the bubble. (c) The construction of  $\Sigma_N$  with  $m=1, n=0$  permits us to extract the signal associated to the first pulse. Moreover, by adjusting the constant dephasing  $\delta$ , it is possible to separate the speaker's response ( $\delta=0$ ) from the bubble's response ( $\delta=\pi/2$ ). (d) The same procedure with  $m=0, n=1$  permits us to extract the signal due to the second pulse.

the acoustic signal of the bubble. In an aquarium filled with water, a bubble is caught up under a net. This use of a net was previously checked not to modify the acoustic response of the bubble [12,13].

The acoustic pulses are generated with an underwater speaker and the pressure is measured with a hydrophone. Both these pieces of apparatus are linked, each via an amplifier, to an acquisition board (NI PCI-4451).

#### A. Phase detection

The extra pressure generated by the oscillations of the bubble is proportional to the real part of  $\alpha$  [17]. From (16) and (19) we thus expect a ratio {conjugated signal over direct signal} of the order of  $(|y_{02}|/6\gamma)\omega_0\Delta t_2$ . Given the pressure amplitudes we are able to obtain experimentally, this ratio is of the order  $10^{-2}$ – $10^{-1}$ . The straight measurement of the conjugated component is therefore impossible for it is totally occulted by the direct component. But we can profit from the fact that both components bear different phases. While  $x_1$  is proportional to  $\sin(\omega_0 t + \varphi_1)$  [see (8b) and (16)],  $x_{pc}$  is proportional to  $\sin(\omega_0(t-2\tau) + \omega_2\tau + \varphi_2 - \varphi_1)$  [see (8b) and (18)]. In order to select a particular component and extract it from the overall  $x_{1+2}$  signal, we used the following trick. Let us submit the bubble to a set of  $N$  two-pulse sequences, with phases  $\varphi_1$  and  $\varphi_2$  randomly varied from one sequence to the other. Let  $\varphi_{1i}, \varphi_{2i}$  and  $s_i(t)$  respectively be the phases of applied pulses 1, 2 and the corresponding hydrophone signal in the  $i$ th sequence. We construct the quantity

$$\Sigma_N(t) = \sum_{i=1}^N s_i(t) \cos(\omega_0 t + \theta_i), \quad (20a)$$

where  $\theta_i$  is a reference phase which is varied from a sequence to the other as

$$\theta_i = m\varphi_{1i} + n\varphi_{2i} + \delta, \quad (20b)$$

with integers  $m, n$  and adjustable dephasing  $\delta$  given once for all (i.e., independent of  $i$ ). Let us suppose for instance that we wish to select component  $x_1(t)$ : we simply have to set  $m=1, n=0$  and  $\delta=\pi/2$ . To select component  $x_{pc}(t)$ , we have to set  $m=-1, n=+1$  and  $\delta=\pi/2+(2\omega_0-\omega_2)\tau$ . It is also possible to select the exciting pulses generated by the speaker: for instance, setting  $\theta_i=\varphi_{1i}$  (i.e.  $m=1, n=0, \delta=0$ ), we select the first pulse, and so on.

In any case, setting parameters  $(m, n, \delta)$ , we select one particular component of the hydrophone's signal, and function  $\Sigma_N(t)$  is then the sum of two quantities: (i) a constant quantity proportional to  $N$  and to the amplitude of the selected component, and (ii) a (constant or  $2\omega_0$ -oscillating) quantity proportional to  $\sqrt{N}$  and to the total amplitude of the unselected components.

Thus the extracting efficiency of such a phase-detection method grows like  $\sqrt{N}$ . Consequently, we need for example  $N=10\,000$  sequences to extract a particular component which is 100 times weaker than the overall hydrophone's signal. Our detection method is illustrated (and checked) in Fig. 3, and applied in Sec III B to the measurement of the phase-conjugated component  $x_{pc}$ .

#### B. Measurement of the phase-conjugated component

Let us capture under the net a bubble with  $T_0=2\pi/\omega_0=0.88\pm 0.01$  ms [18]. We then submit it to a series of 3000 two-pulse sequences: the first pulse with a period  $T_1=0.88$  ms ( $=T_0$ ) and a duration  $\Delta t_1=15$  ms, and the second pulse with a period  $T_2=0.44$  ms ( $=T_0/2$ ) and a duration  $\Delta t_2=10$  ms. In order to have the strongest signal possible,

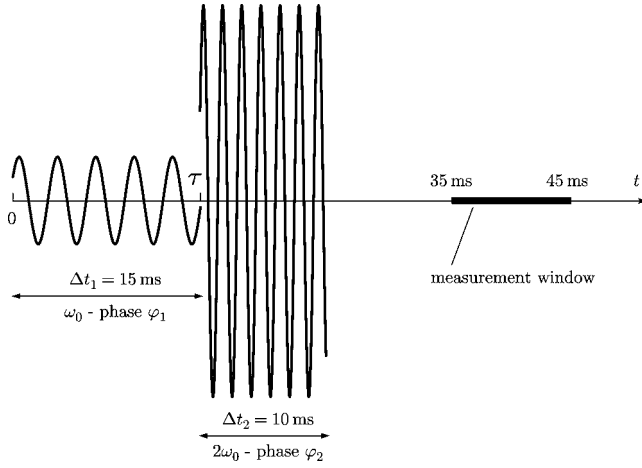


FIG. 4. A sequence of measurement. The bubble is first excited from  $t=0$  by a resonant ( $\omega_1=\omega_0$ ) pulse during 15 ms. Then a large-amplitude  $2\omega_0$  pulse is applied during 10 ms. We acquire the hydrophone's signal from  $t=35$  to 45 ms. This sequence is repeated  $N$  times, with phases  $\varphi_1$  and  $\varphi_2$  randomly varied from one sequence to the other.

we initiate the second pulse at  $\tau=\Delta t_1$ , i.e., we perform the parametric excitation immediately after the end of the direct excitation (see Fig. 4), with an amplitude  $|y_{02}|=(1.23\pm 0.03)\times 10^{-2}$  for the second pulse.

We start to measure the pressure when the hydrophone's signal is low enough to be unsaturated (10 ms after the end of the second pulse) and we stop the acquisition 10 ms later. From this signal, we then construct function  $\Sigma_N(t)$ . By setting  $m=1$ ,  $n=0$ , and looking for the value of  $\delta$  which maximizes the amplitude of  $\Sigma_N$ , we obtain the envelope of the direct component  $x_1(t)$  (Fig. 5). We then consider the limit of significance of any extracted signal to be this direct envelope divided by  $\sqrt{N}$ : the  $\Sigma_N(t)$  function we obtain with a particular

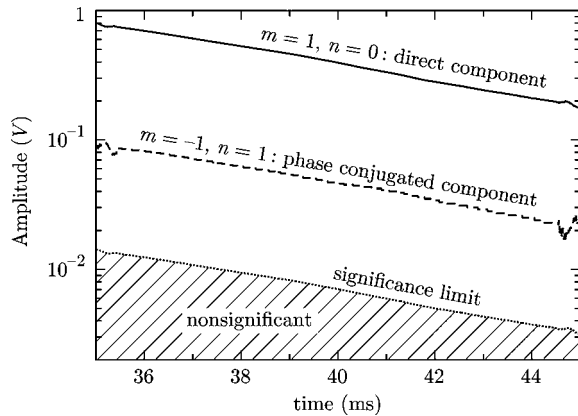


FIG. 5.  $\Sigma_N(t)$  for different settings of  $(m, n)$ . For  $m=1$ ,  $n=0$ , we obtain the envelope of the direct component, with an exponential decay as expected (note the logarithmic scale in the figure). The limit of significance of any detected signal is then considered to be this direct envelope divided by  $\sqrt{N}$ : any combination of phases yielding a  $\Sigma_N(t)$  signal lower than this limit is nonsignificant. We find that, for  $(m=-1, n=1)$ ,  $\Sigma_N$  is over the significance limit: phase conjugation is actually observed.

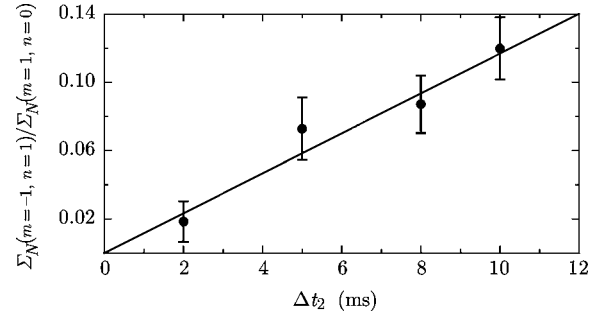


FIG. 6. Ratio of the conjugated and direct components as a function of the duration  $\Delta t_2$  of the second pulse, for a fixed amplitude  $|y_{02}|=1.23\pm 0.03\times 10^{-2}$ . Error bars correspond to  $1/\sqrt{N}$ . The linear fit gives a slope of  $1.17\pm 0.08\times 10^{-2}$  for an expected value of  $(\pi/3\gamma)(|y_{02}|/T_0)=(1.06\pm 0.04)\times 10^{-2}\text{ ms}^{-1}$ .

combination of  $m$  and  $n$  is considered as nonsignificant unless it overshoots this limit. We can check in Fig. 5 that, for  $(m=-1, n=1)$ ,  $\Sigma_N(t)$  is over this limit, which confirms the existence of the conjugated component due to the bubble. In Figs. 6 and 7, we also check the linear dependences of this signal with duration  $\Delta t_2$  and amplitude  $|y_{02}|$  of the second pulse.

Note that in this experiment, our assumption of small oscillation amplitudes is valid. We can check it by measuring the extra pressure generated by the bubble. It may seem surprising, as we excite the bubble at both its direct and parametric resonances. In fact, in both cases, damping severely limits the amplitude of the oscillations. For the direct resonance, we can calculate from Eq. (14) that  $|x|\approx(Q/3\gamma)|y|$  where  $Q$  is the quality factor of the oscillator. For a millimetric bubble,  $Q\sim 30$ . So, even with  $|y|\sim 10^{-2}$  (i.e., the highest pressure amplitude we are able to generate in our experiment), we expect  $|x|\sim 10^{-1}$ . As concerns the parametric resonance, we can calculate from Eq. (15) that the threshold for the parametric instability is  $3\gamma/Q\sim 10^{-1}$ . As our excitation amplitude is lower than this threshold, the oscillations of the bubble remain low.

#### IV. DISCUSSION

Let us now come back to our comments about Eq. (19) which we postponed above. At time  $t=2\tau$ , the phase of  $\alpha_{pc}(t)$

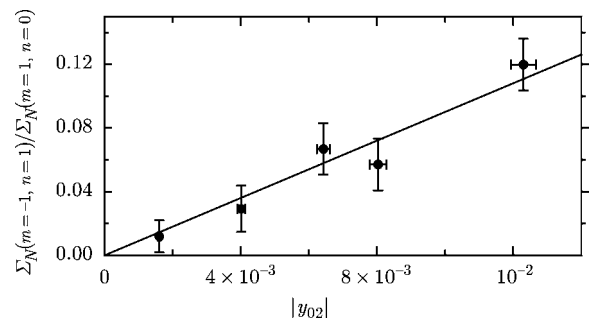


FIG. 7. Ratio of the conjugated and direct components as a function of the amplitude  $|y_{02}|$  of the second pulse, for a fixed duration  $\Delta t_2=10$  ms. Error bars correspond to  $1/\sqrt{N}$ . The linear fit gives a slope of  $(9\pm 1)\times 10^{-5}$  whereas the expected value is  $(\pi/3\gamma)(\Delta t_2/T_0)=(8.6\pm 0.1)\times 10^{-5}$ .

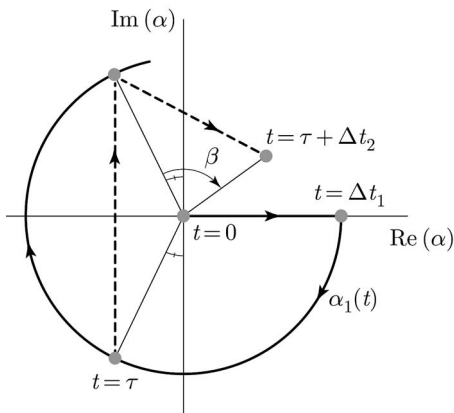


FIG. 8. Trajectory of the  $\alpha$  variable in the complex plane, neglecting damping. From  $t=0$  to  $t=\Delta t_1$ , the bubble is excited by the first pulse. The subsequent free oscillations correspond to a circular movement in the complex plane. At  $t=\tau$ , the parametric excitation generates a component which is proportional to  $\alpha^*$  (vertical dotted arrow) multiplied by a fixed complex number (second dotted arrow). This process is analogous to a spin-flip in NMR.

is independent of the value of  $\omega_0$ . If then not a single bubble, but a whole cloud of (noninteracting) bubbles with slightly different radii (and therefore slightly different values of  $\omega_0$ ) is excited at times  $t=0$  and  $t=\tau$  by the above-described two-pulse acoustic sequence, then a refocusing of their phases should occur at time  $t=2\tau$ . This refocusing should generate a local extra pressure signal in the water. Such a bubble echo is formally analogous to the spin echo of the NMR domain. This can be visualized in the complex plane of variable  $\alpha$ , as displayed in Fig. 8. As a matter of fact, there is a strong analogy between our variable  $\alpha$  and the transverse magnetization  $\vec{m}_\perp$  (i.e., the component perpendicular to the static magnetic field  $\vec{B}_0$ ) of the spin in the NMR domain. In this analogy, the complex plane of variable  $\alpha$  (which is in fact the phase-space of the bubble's oscillation) should be paralleled with the NMR transverse plane (orthogonal to  $\vec{B}_0$ ). Initially the bubble is at rest:  $\alpha(t=0)=0$ . After the first pulse, the bubble is excited:  $\alpha(t=\Delta t_1) \neq 0$  (by care of simplicity, we have substituted a straight line for the true path of  $\alpha$ —in fact a spiral—between times  $t=0$  and  $t=\Delta t_1$ ). Then, between times  $t=\Delta t_1$  and  $t=\tau$ , the bubble oscillates freely: (still neglecting dissipation)  $\alpha$  follows a circle, exactly as the tip of the transverse magnetization does in NMR during the Larmor precession around field  $\vec{B}_0$ . The effect of the second pulse is described by Eq. (15) which, when using variable  $\alpha$ , reads

$$\dot{\alpha} = \alpha^* \left( \frac{-i\omega_0 |y_{02}|}{3\gamma} e^{-i(\omega_2 t + \varphi_2)} \right). \quad (21)$$

The parametric excitation associated with the second pulse therefore generates a component of  $\alpha$  which is proportional to  $\alpha^*$ . This effect is symbolized by the vertical dotted arrow in Fig. 8 and can be paralleled with the result of the  $\pi$  pulse in the analogous NMR sequence. Observe that the upshot of the second pulse is not mathematically speaking a pure complex conjugation, due to the multiplication of  $\alpha^*$  by the com-

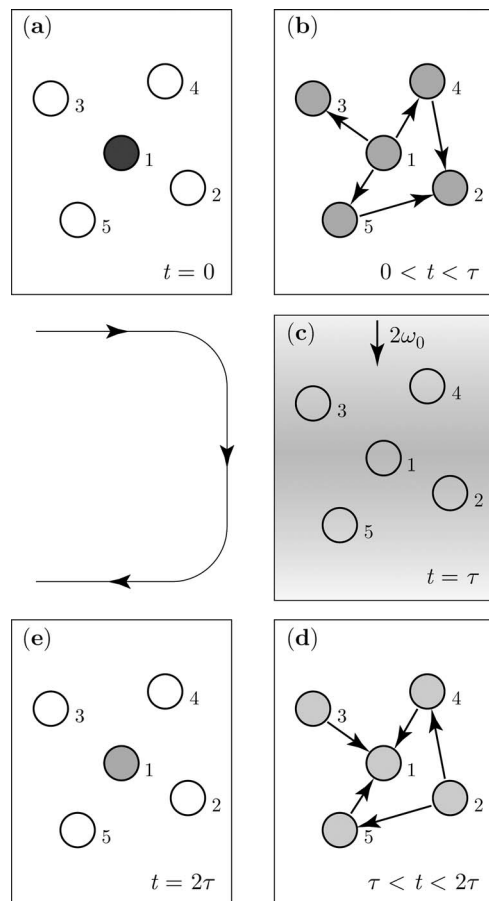


FIG. 9. Phonon echoes in a bubbly liquid. (a) A single bubble (1) is excited at  $t=0$ : bubble 1 starts oscillating. (b) A few scattering paths originating in bubble 1: bubble excitation is spread all around bubble 1 by multiscattering. (c) A strong  $2\omega_0$  pulse is applied to the cloud at  $t=\tau$ : bubble oscillations are partially phase conjugated. (d) Reversed scattering paths of (b): phase conjugation acts like a time reversal. (e) The phase-conjugated component is refocused on bubble 1 at  $t=2\tau$ .

plex number between parentheses in the right-hand side of Eq. (21), which is symbolized by the skew dotted arrow in Fig. 8. Nevertheless the effect is the same since the argument  $\beta = -\pi/2 - \omega_2 \tau - \varphi_2$  of this multiplying factor is independent of  $\omega_0$ .

If the bubbles of the cloud were uncoupled, one could then observe bubble echoes analogous to spin echoes in NMR. But, contrary to spins, bubbles are generally strongly coupled together, due to the slow dying out (like  $1/r$ ) of the pressure field generated by oscillating bubbles. Unless extremely dilute bubble clouds are used, interactions are likely to play an important role and it is noteworthy that the possibility of observing bubble echoes has already been envisaged in literature [14], but only with neglected bubble interactions. In fact, as illustrated in Fig. 9, multiscattering effects associated with bubble interactions could be turned to profit to observe echoes in the following way. Let us consider a monodisperse bubble cloud and suppose that, at time  $t=0$ , we excite a *single* bubble, say bubble 1 [Fig. 9(a)]. This bubble starts oscillating and generates a (spherical) sound wave. This sound wave will in turn excite neighboring

bubbles and so on. All bubbles being assumed to have roughly the same Minnaert angular frequency  $\omega_0$ , a strong (resonant) multiscattering spreads excitation all around bubble 1 [Fig. 9(b)]. Let us now suppose that a  $2\omega_0$ -oscillating extra pressure is applied to the whole cloud at time  $t=\tau$  [Fig. 9(c)]. Each bubble of the cloud will then undergo a (partial) phase conjugation, as explained in the present paper. With respect to multiscattering, this second acoustic pulse will start a time-reversal [Fig. 9(d): note the change of all the scattering paths direction arrows with respect to Fig. 9(b)] and the phase-conjugated component of the multiscattered wave will be refocused on bubble 1 at time  $t=2\tau$  [Fig. 9(e)]. Such an acoustic boomerang effect is known as a phonon echo and has been already observed in piezoelectric powders [15].

## V. CONCLUSION

Introducing complex variable  $\alpha$ , we have obtained a very simple equation to deal with the resonant direct  $\omega_0$  excitation

as well as parametric  $2\omega_0$  excitation of a bubble with Minnaert angular frequency  $\omega_0$ . The latter parametric excitation involves a phase conjugation mechanism, the conjugated component being weak but bearing a specific phase. We have observed and measured the conjugated signal with a single bubble undergoing a two-pulse acoustic sequence: the first pulse with angular frequency  $\omega_0$  directly excites the bubble's oscillation whereas the second pulse with angular frequency  $2\omega_0$  induces the phase conjugation. This effect could be used to produce bubble echoes, provided that the bubble-bubble interaction be properly turned to account.

## ACKNOWLEDGMENTS

We thank Nicholas Beck for his contribution to the English version of this paper.

- 
- [1] F. V. Bunkin, Y. A. Kravtsov, and G. A. Lyakhov, *Sov. Phys. Usp.* **29**, 607 (1986).
  - [2] E. A. Zabolotskaya, *Sov. Phys. Acoust.* **30**, 462 (1984).
  - [3] A. O. Maksimov, *Sov. Phys. Acoust.* **35**, 53 (1989).
  - [4] L. M. Kustov, V. E. Nazarov, and A. M. Sutin, *Sov. Phys. Acoust.* **31**, 517 (1985).
  - [5] L. M. Kustov, V. E. Nazarov, and A. M. Sutin, *Sov. Phys. Acoust.* **32**, 500 (1986).
  - [6] N. P. Andreeva, K. Karhiev, and L. M. Sabirov, *Sov. Phys. Acoust.* **37**, 425 (1991).
  - [7] O. Y. Butkovskii, E. A. Zabolotskaya, Y. A. Kravtsov, and V. V. Ryabykin, *Sov. Phys. Acoust.* **33**, 104 (1987).
  - [8] S. T. Zavtrak, *Phys. Rev. E* **51**, 2480 (1995).
  - [9] M. Minnaert, *Philos. Mag.* **16**, 235 (1933).
  - [10] T. Leighton, *The Acoustic Bubble* (Academic Press, London, 1994).
  - [11] R. J. Glauber, *Phys. Rev.* **131**, 2766 (1963).
  - [12] P.-Y. Hsiao, M. Devaud, and J.-C. Bacri, *Eur. Phys. J. E* **4**, 5 (2001).
  - [13] V. Leroy, M. Devaud, and J.-C. Bacri, *Am. J. Phys.* **70**, 1012 (2002).
  - [14] S. Lopatnikov, *Sov. Tech. Phys. Lett.* **6**, 270 (1980).
  - [15] C. Frénois, J. Joffrin, and A. Levelut, *J. Phys. (Paris)* **34**, 453 (1973).
  - [16] Note that the isentropic evolution assumption is very good for millimetric radius bubbles we use in our experiments. Nevertheless, to account for thermal exchanges, a polytropic exponent  $\kappa$  (instead of  $\gamma$ ) can be introduced (see, e.g., Ref. [10], pp. 175–181).
  - [17] More precisely, the oscillation of the bubble generates an extra pressure  $p$  which reads, at a distance  $r$  and neglecting propagation,  $p=\rho(R_0^3/r)\ddot{x}$  [see, e.g., formula (2) in [12]]. In the present case of a harmonic oscillation with angular frequency  $\omega_0$ , one has  $\ddot{x}=-\omega_0^2x$ .
  - [18] Note that, at this frequency, the acoustic wavelength is very large compared with the radius of the bubble. Hence, both assumptions of incompressible water and spherical deformations of the bubble are valid.